

Wide area monitoring system control management of the IEEE-14 bus system using least square support vector regression

Lilik Jamilatul Awal¹, Syahirah Abd Halim², Nor Azuana Ramli³, Jafferi Bin Jamaludin⁴,
Mohd Syukri Ali⁴

¹Department of Electrical Engineering, Faculty of Advanced Technology and Multidicipline, Airlangga University, Surabaya, Indonesia

²Department of Electrical Electronic and Systems Engineering, Faculty of Engineering and Built Environment,
Universiti Kebangsaan Malaysia, Bangi, Malaysia

³Centre For Mathematical Sciences, Universiti Malaysia Pahang, Pekan, Malaysia

⁴Higher Institution Centre of Excellence (HiCoE), UM Power Energy Dedicated Advanced Centre (UMPEDAC), Level 4, Wisma R&D,
University of Malaya, Kuala Lumpur, Malaysia

Article Info

Article history:

Received Oct 6, 2021

Revised May 15, 2022

Accepted Jun 13, 2022

Keywords:

IEEE 14-bus system

Least square support vector
regression

Mean square error

Phasor measuring units

Reliable energy

Wide area monitoring systems

ABSTRACT

The wide area monitoring system (WAMS) records and monitors every fault or disturbance that occurs in a power system network using phasor measuring units (PMUs). Extensive monitoring of the condition of the electrical power system can ensure the sustainability of reliable energy. The accuracy of the PMUs placement can be determined using the least square support vector regression (LS-SVR) technique. The primary goal of this study is to assess the level of accuracy of the PMUs placement using mean square error (MSE). First, the IEEE-14 bus system equipped with PMUs was built in Matlab software using Simulink. The MSE of the PMUs was then calculated using the LS-SVR. The results revealed that the lower the MSE, the better the PMUs placement. It was also observed that placing the PMUs on bus 2, bus 6, and bus 9 produced the lowest value of MSE.

This is an open access article under the [CC BY-SA](https://creativecommons.org/licenses/by-sa/4.0/) license.



Corresponding Author:

Lilik Jamilatul Awal

Department of Electrical Engineering, Faculty of Advanced Technology and Multidicipline

Airlangga University

Street of Mulyorejo, Surabaya 60155, Indonesia

Email: lilik.j.a@ftmm.unair.ac.id

1. INTRODUCTION

The power grid is a technology that comprises of a transmission line network, control devices, and energy monitoring. The first electricity grid system was installed in great barrington, Massachusetts, in 1886. It was a one-way interaction or unidirectional system at the time, with a modest need for power. With the growth of technology and industry, the need for power is growing. As a result, the grid is outfitted with two-way communication, allowing the grid to adapt to the ever-changing power system. The supervisory control and data acquisition system (SCADA) and energy management system (EMS) manage this smart grid technology [1]. However, SCADA and EMS have poor data upload rates and cannot provide the greatest level of smart grid efficiency.

Ree *et al.* [2] the invention of the synchronized global positioning system, also known as global positioning system (GPS), aided the synchronized-measurement technology in the establishment of a wide-area monitoring system (WAMS). The understanding of WAMS in reference [3]–[9] can summarize as a network technology that uses modern and digital measuring devices, a control system, and a communication device to operate a power system. WAMS consists of three dependent substations, namely management, measurement, and communication. Despite the fact that the functioning is different, the architecture of such

substations is nearly similar. This technology is used to monitor smart grid parameters like voltage and phasor and to speed up network calculations. The operation of the power system is continually monitored by this technology, and real-time data of high quality is provided to detect unusual activities or interruptions. When the problem or fault occur on the WAMS appear as a one of the solutions to manage the reliable energy. In the recent years, focusing on fault location method have been improved by some researcher which mention in papers [10]–[13]. Awalin *et al.* [10] was contribute fault detection on the distribution network based on voltage and current measurement by using matching approach combine with impedance-based method. Based on this research, the result shows that this paper was obtained the acceptable accuracy. By using matching approach, Awalin *et al.* [11] was compare the accuracy by using different simulation tools namely, diligent and power system computer aided design (PSCAD) simulation program. From this study it is found that digsilent has a higher level of accuracy compared to PSCAD if the location of the disturbance using a matching approach. However, the authors mention that this may not be the case if applied using other interference location methods. While the paper Idris *et al.* [12] has also examined the location of interference by using data from two different terms to detect interference in the transmission system. Awalin *et al.* [13] focuses on how to detect the types of disturbances that occur in electrical power distribution systems.

Wang *et al.* [14] mention that the hierarchical structure of WAMS is consist of main network with multiple of another network. Gore and Kande [4], the data that collected from phasor measuring unit (PMU) will be send through every network of communication, then the collected data is send to phasor data concentrators (PDC). Similar paper Fesharaki [15] mention that PDC process the data from PMU for operation of WAMS with time-stamp provided by GPS. Most of the latest data is lost due to PDC or communication failure. Based on paper [16], the resynchronize data that measured from PMU and process the phasor difference result which are used in real time control is the main function of PDC. The minimizing of bandwidth between control site and PDC, need higher input information than output. Other purposes of PDC are additional monitoring from system, commands of operation and commands of maintenance to data packet. The phasor data that receive from PMU are saved. The first PMU is installed at Scherer, Georgia in 1992. This test involves 500 kV lines of opening at Klondike and closing at Bonaire. Kamwa *et al.* [17] the PMUs is located at plant Scherer and five other places in Tennessee, Georgia, and Florida.

Various PMU placement methods was observed in papers [18]–[23] in order to optimize the number of PMU placement and the power electrical delivery. The PMU used to monitor the post ever in early manufacturer because of the communication channel is very expensive. Another research about PMU in paper [24] mention the PMU data can undergo the transferring 10 to 100 Hz by implementation of additional control of damping. The PMU is used to divide the fundamental frequency and obtain the phasor representation. Pahasa and Ngamroo [25], by using the non-recursive update type discrete fourier transform (DFT) on the sample data, the phasor representation can be determined. The antialiasing filter is injected that can limit the bandwidth and resulting less data sample. The DFT can eliminate harmonic of the sample signal. Somehow, the error of estimation of phasor is present by nonharmonic signal and noise. WAMS was used to improve the protection and control of smart grids. Phadke and Thorp [26], prior to the introduction of WAMS, a system known as the power system frequency monitoring network (FNET) was developed in 2004 as a pioneer WAMS.

On the other hand, support vector machine (SVM) is the way to solve the quadratic programing problem. The support vector can be used to solve the estimation problem by employing Vapnik's epsilon insensitive loss function and Huber's loss function was discussed in paper [27]. Suykens *et al.* [28], the interdisciplinary topic of least squares support vector machines (LS-SVM) are include neural network, data mining, pattern recognition, machine learning, optimization, system control, signal processing, statistics, mathematics and linear algebra

Suykens *et al.* [29], the support vector can be used to solve the estimation problem by employing Vapnik's epsilon insensitive loss function and Huber's loss function. Suykens *et al.* [30], WAMS is also known as a sensor network because there are many sensors involved, such as PMUs and current sensors. These sensors transmit real-time dynamic data, which is usually protected from malicious attacks by encryption algorithms, over wide-area networks (WANs) to power system control centres, allowing monitoring and control of the entire system.

Some publications have been reviewed, which employ least square support vector regression (LS-SVR) method to tackle the research problem. Gangil and Narvey [31], the support vector regression (SVR) algorithm is based on the SVM and can handle nonlinear regression problems. Based on the findings reported in [32], SVR can obtain a hyperplane that can assist in forecasting the distribution of information properly. SVM, on the other hand, is used as a strong mathematical foundation. SVM determines the plane used to categorise the data. SVR can represent non-linear relationships, give a unique and global solution, and provide a more generic answer while avoiding forced training.

On the other hand, SVR can efficiently process input vectors with large dimensionality to produce a global solution as mention in paper [33]. When dealing with high-dimensional input vectors, the weight

numbers of an artificial neural network (ANN) are greater. Under the identical testing conditions, SVR technique outperforms ANN. The weights are tuned, and the process is repeated with various primary or initial values, which may result in a non-global solution. To solve the regression problem, SVR employs quadratic programming (QP).

According to publication papers [34], [35] introduces the least square support vector regression (LS-SVR) as one of the regression tools. LSSVR has been widely applied to solve various problems, such as to detect water temperature discussed in the paper [34]. The WAMS receives signals in the form of electric energy from various areas based on the function that has been determined at the WAMS. The LS-SVR is a reformed version of SVR that uses a set of linear equations to determine the regression. When compared to quadratic programming, linear equations are easier to solve. This demonstrates that LS-SVR requires less processing time than SVR. As indicated in publication [30], the karush-kuhn-tucker (KKT) is used in LS-SVR. LS-SVR is also based on the determination of parameter γ and σ^2 values. Inequality constraints are employed in place of inequality constraints. Gordon and Tibshirani [36], the general solution of LS-SVR is derived from the square loss function of N data and the function of quadratic penalty.

Jung [37], there are two drawbacks of LS-SVR: the equality requirement causes the solution to become sparse, and the solution is not robust to outliers. All parameters are required to generate a solution in the absence of a sparse solution. A pruning approach is used to solve problems with sparse solutions. Meanwhile, the weighted LS-SVR is then used to reduce the effect of the outliers. Synchrophasor measuring units, also known as synchrophasors, are devices that give time-synchronized data on power system operating states according to [38]. It was launched in the early 1980s and has evolved in tandem with the advancement of technology throughout the world, as stated by [39].

This synchronised measurement can help to avoid significant blackouts and a lack of time-synchronized high-resolution data. A blackout can occur as a result of a breakdown and increased demand during peak hours, whereby the power generated by the facility is insufficient to meet the demand. This might have an impact on a country's economy. Without GPS, synchrophasors can monitor and post data analysis when data have been saved locally, but there is no wide-area connection. However, PMUs can remotely monitor and operate applications. Centeno *et al.* [40], examples of applications include voltage stability assessment, islanding detection, oscillation monitoring, and state estimation using GPS technology. The system's functionality may be improved by employing PMUs since measurements are made in real time and data can be retrieved online.

WAMS was employed as the control management of the institute of electrical and electronics engineers (IEEE)-14 bus system. In this study, based on least square support vector regression. In general, WAMS controls, monitors, and operates the power system in conjunction with the communication system and metering devices such as PMUs. The signal from a limited region may be sent to the control panel using this technique.

Meanwhile, the LS-SVM regression technique is known as LS-SVR. In this study, the LS-SVR is employed to determine the level of accuracy of PMUs placement in the IEEE-14 bus system based on mean square error (MSE). This paper has been organized as follows. In the following section, a methodology is presented by explain LS-SVR the model of tested network. The results of the proposed method are presented and discussed in section 3. Finally, conclusions are drawn in section 4.

2. METHOD

Figure 1 depicts the technique used in this study. It shows the process flowchart for controlling the IEEE-14 bus system's WAMS using LS-SVR. To begin, the IEEE-14 bus system was designed with Simulink in Matlab software. This IEEE-14 bus system is made up of two alternating current (AC) generators, three synchronous compensators, and five transformers. The IEEE-14 bus system parameters were added into the circuit. Qian *et al.* [16], the PMU is located at bus 2, bus 6, and bus 9. The amplitude of V_{abc} , phase of V_{abc} , and frequency of V_{abc} were then selected as the outputs of the PMU. However, the PMU output, which is the magnitude of V_{abc} at buses 2, 6, and 9, is inserted in LS-SVR. The MATLAB software created the LS-SVR parameters, namely gamma and sigma. PMU 1 is the PMU at bus 2, bus 6, and bus 9. Next, the value of MSE for PMU 1 was acquired. The PMU was then assigned to bus 1, bus 3, bus 4, bus 5, bus 7, bus 8, bus 10, bus 11, bus 12, bus 13, and bus 14. The MSE values from PMU 2 to PMU 34 were recorded. The MSE value of each PMU placement were then compared to PMU 1's MSE.

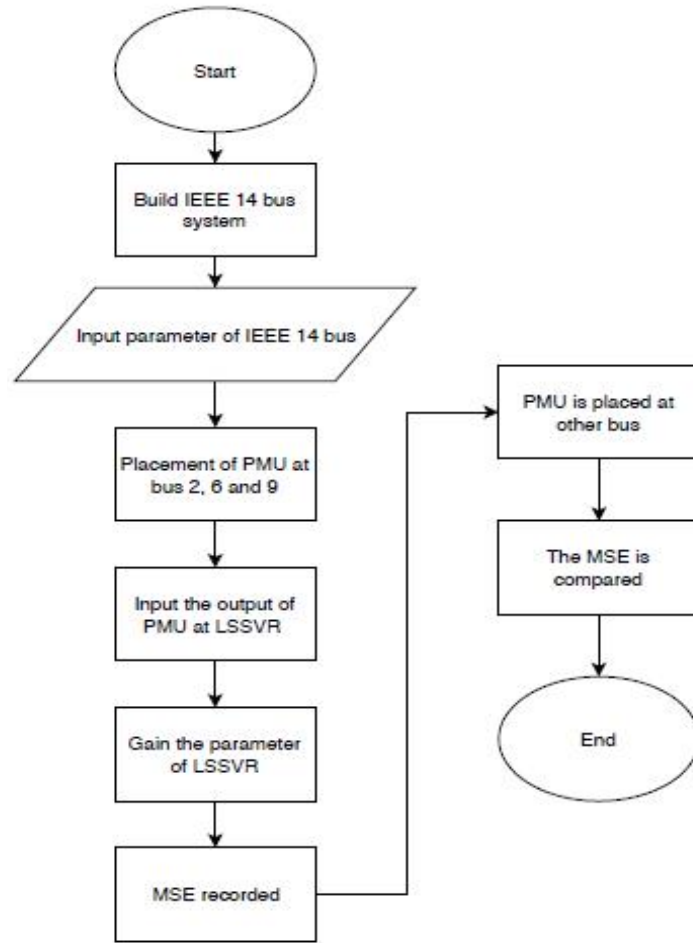


Figure 1. The flowchart

2.1. LS-SVR

The least square support vector regression method is based on least square support vector machine for regression with the KKT conditions for optimality. This is the solution for non-linear programming to be optimal by providing the satisfied of some regularity conditions. Estimation dataset,

$$\{x_i, y_i\} \quad i = 1N \tag{1}$$

vector input = $x_i \in \mathbb{R}^n$
 Corresponding outputs = $y_i \in \mathbb{R}$

for non-linear case,

$$f(x_i) = w^T \phi(x_i) + b \tag{2}$$

where,
 $\phi(\cdot): \mathbb{R}^n \rightarrow \mathbb{R}^d$ is nonlinear map into a higher dimensional feature space and dimensionality d might be infinite (∞).

$w \in \mathbb{R}^d$ is parameter vector.

$b \in \mathbb{R}$ is bias term.

Subjected to the equality constraints:

$$y_i = w^T \phi(x_i) + b + e_i \tag{3}$$

the output of LS-SVR.

$$y(x) = w^T \phi(x) + b + \epsilon_i \quad (4)$$

where, $x \in \mathbb{R}^i, y \in \mathbb{R}, \phi(\cdot): \mathbb{R}^i \rightarrow \mathbb{R}^i$.

The LS-SVM is formulated in primal weight space as (5).

$$(\min) w, b, \epsilon \mathcal{J}(w, \epsilon) = 12w^T w + \gamma \sum_{i=1}^n \epsilon_i^2 = 1 \quad (5)$$

The polynomial of Lagrange duality problem is (6).

$$L(w, b, \epsilon, a) = \mathcal{J}(w, \epsilon) - \sum_{i=1}^n \beta_i N_i [w^T \phi(x_i) + a + \epsilon_i - y_i] \quad (6)$$

By this theory, the $\phi(\cdot)$ is not calculated because the matrix from the quadratic programming problem cannot be define. The Mercer's condition only depended on parameter value of K and θ . The Lagrange functions:

$$L_{LS-SVR} = f(w, b, \epsilon, a) = 12(w^T w) + \frac{\gamma}{2} \sum_{i=1}^N \epsilon_i^2 - \sum_{i=1}^n a_i [w^T \phi(x_i) + b + \epsilon_i - y_i] \quad (7)$$

where b_i is Lagrange multipliers. The conditions for optimality are,

$$\begin{aligned} \frac{df}{dw} &= 0, w = \sum_{i=1}^N a_i \phi(x_i) \\ \frac{df}{db} &= 0, w = \sum_{i=1}^N a_i = 0 \end{aligned}$$

By utilizing mercer condition, $\Omega_{kj} = (\phi(x_k))^T \phi(x_j) = K(x_k, x_j), k, j = 1, 2, \dots, l$. The resulting LV-SVR model for this project as the function estimation is (8).

$$\hat{m}(x) = \sum_{i=1}^N \hat{a}_i K(x, X_i) + \hat{b} \quad (8)$$

The radial basis function (RBF) kernel is used to define K (x, Xi).

$$K(x, X_i) = e^{-\left\| \frac{x - x_i}{2\sigma^2} \right\|^2} \quad (9)$$

LS-SVR model is (10).

$$y(x) = \sum_{i=1}^n a_i K(x, X_i) + b \quad (10)$$

2.2. Model of test system

This circuit is made up of two AC generators, three synchronous compensators, five transformers, and fourteen PMUs. Figure 2 depicts the IEEE-14 bus system test network. According to publication [8], the PMUs are chosen to be installed at bus 2, bus 6, and bus 9. The lowest and highest magnitudes of voltage for phases a, b, and c are recorded. These values are then sent into the LS-SVR. Figure 3 is an example of a PMU placement at bus 2. PLL PMU is used as the PMU model while V_{abc} at the bus is the PMU's input. The PMU input data is given by the values of magnitude, phase angle, and frequency of V_{abc} . The PMU is installed on the IEEE-14 bus system, located at bus 1 to bus 14. The PMU output consisting of the amplitude of V_{abc} at the bus is recorded and sent into the LS-SVR software. The LS-SVR then produces MSE at each PMU placement. Figure 2 shown the design circuit of IEEE 14 bussystem. The PMU are placed at bus 2, bus 6 and bus 9 according to paper [9]. The minimum and maximum magnitude of voltage phase a, b, c are recorded. These values are used as the input of LS-SVR.

Figure 3 shown the example of one PMU placement at bus 2. The PLL PMU is used as the PMU model. The V_{abc} at bus is the input of PMU. The output of PMU given as magnitude of V_{abc} , phase angle and frequency. The overall PMU placed at IEEE 14 bus system which are at bus 1 until bus 14 is illustrated in Figure 4. The output of PMU is recorded. The magnitude of V_{abc} at bus is recorded and became the input of LSSVR program. The LS-SVR gave output of MSE at all PMU placements.

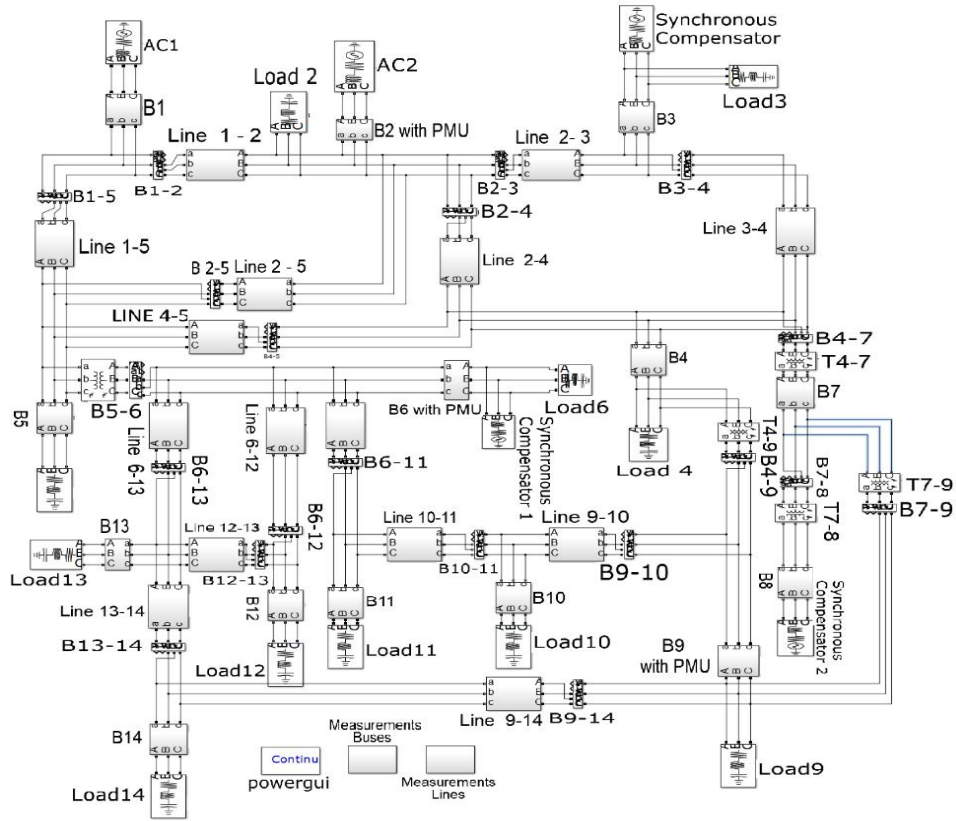


Figure 2. The IEEE 14 bus with PMU placement at bus 2, bus 6 and bus 9

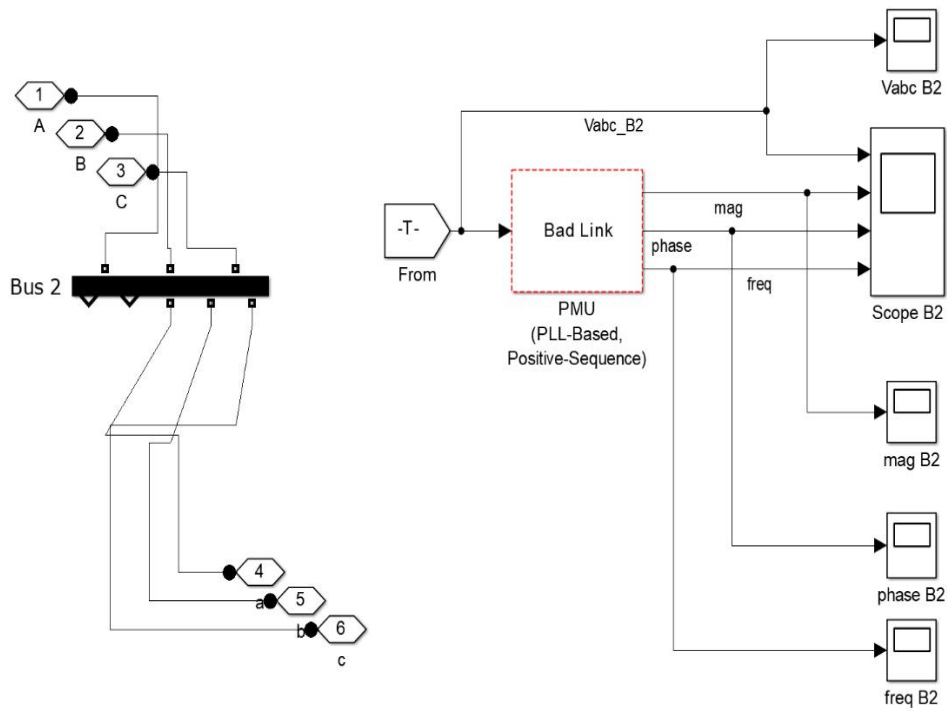


Figure 3. The PMU placement at bus 2

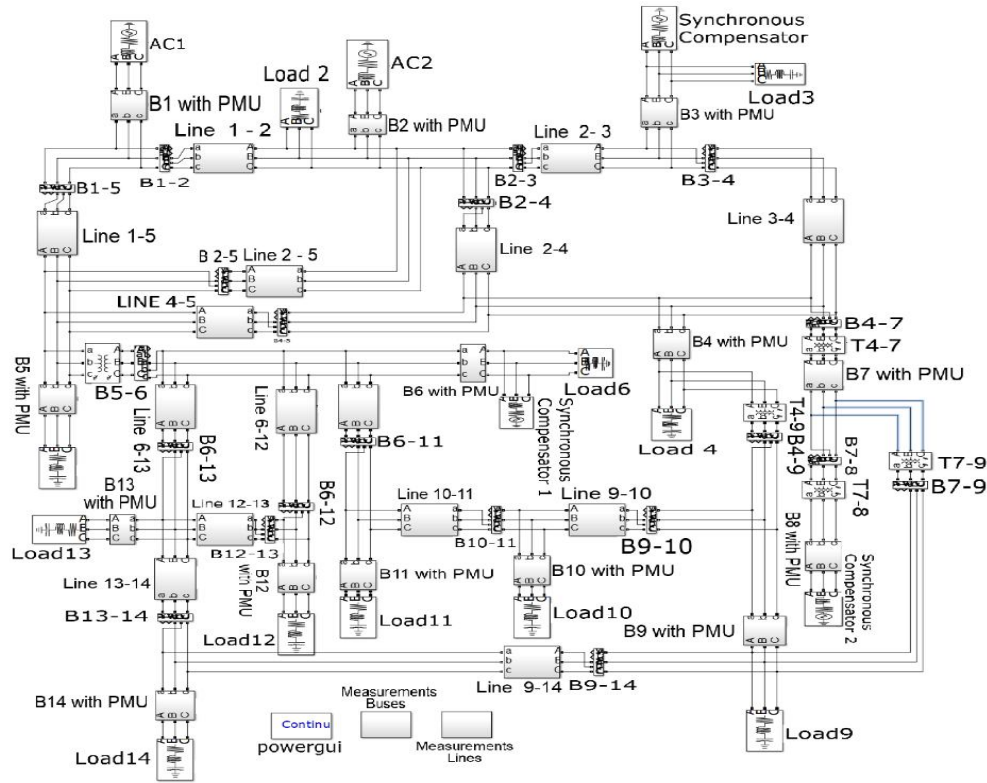


Figure 4. The IEEE 14 bus system with PMU placement at all bus

3. RESULT AND DISCUSSION

The locations of the PMU at all buses were adopted from paper [8]. It was compared to the ideal placement of the PMU. The LSSVR was developed using the MATLAB programming language. The MSE was computed using the developed code for LSSVR. The MSE data were then compared to the location of other set of PMU.

3.1. Simulation result of PMU

The simulation results from each PMU's measurement are detailed in this section. Following the lead of paper [8], one of many PMU designs was installed at bus 2, bus 6, and bus 9. The simulation data when the PMU was installed at all buses was acquired by utilizing the MATLAB software. The simulation data may be acquired using the MATLAB software, as shown in Figures 5, 6, and 7. Figures 5, 6, and 7 depict the magnitude of voltage at phases a, b, and c, which were recorded at buses 2, 6, and 9, respectively.

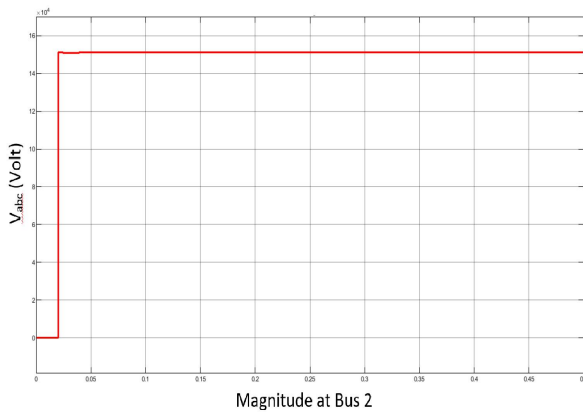


Figure 5. The magnitude of V_{abc} at bus 2

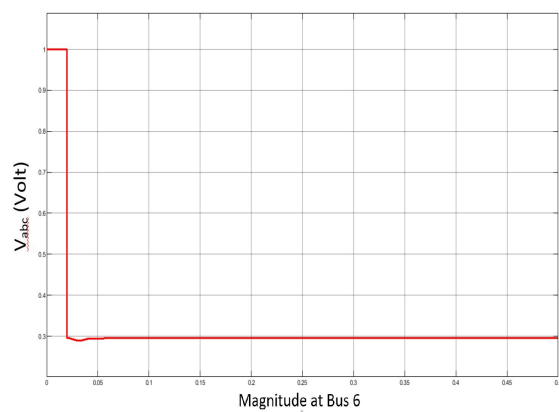


Figure 6. The magnitude of V_{abc} at bus 6

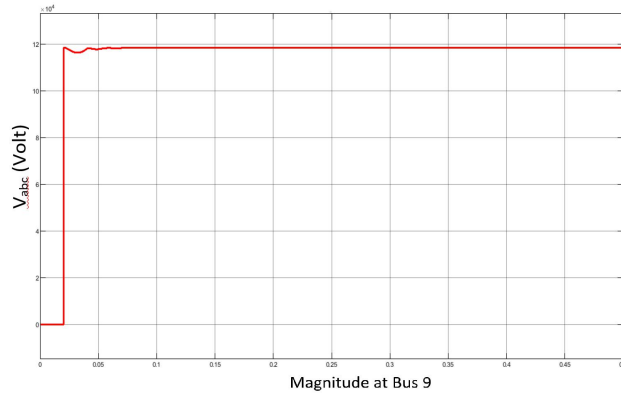


Figure 7. The magnitude of V_{abc} at bus 9

As an example, Figure 5 depicts the amplitude of V_{abc} at bus 2. This magnitude is achieved by positioning the PMU at bus 2. The output of the PMU was voltage, frequency, and phase of V_{abc} . However, only the magnitude of voltage at phases a, b, and c was employed in this study. In MATLAB programming, the maximum and minimum magnitudes of V_{abc} at bus 2 were utilised as inputs to LS-SVR. The maximum and minimum value of the magnitude of V_{abc} are $1.512e+05V$ and $1.000e+00V$ respectively.

The amplitude of V_{abc} at bus 6 is seen in Figure 6. This magnitude is obtained by positioning the PMU on bus 6. The output of the PMU was voltage, frequency, and phase of V_{abc} . However, only the magnitude of voltage at phases a, b, and c is employed in this study. In MATLAB programming, the maximum and minimum magnitudes of V_{abc} at bus 6 were utilised as inputs to LS-SVR. The magnitude of V_{abc} has maximum and minimum values of $1.000e+00$ and $2.894e-01$, respectively.

Figure 7 depicts the amplitude of V_{abc} at bus 9. This magnitude was acquired by connecting the PMU to bus 6. The PMU output was voltage, frequency, and phase of V_{abc} . However, the magnitude of voltage at phases a, b, and c is solely employed in this study. In MATLAB programming, the maximum and lowest magnitudes of V_{abc} at bus 9 were used as the input of LS-SVR. The highest and lowest magnitudes of V_{abc} are $1.186e+05$ and $1.000e+00$, respectively. Table 1 displays the values for the lowest and maximum voltages on phases a, b, and c simulated at bus 2, bus 6, and bus 9. Table 1 displays the data derived from measurements taken at several buses. The first column is the PMU placement, which is categorized depending on PMU placement. The minimum and maximum values of V_{abc} 's magnitude are critical for calculating the MSE of PMU placement. In addition, Table 1 is utilized to present for further computation. Column 2 contains information on the minimum voltage values of phases a, b, and c. Since bus 6 is interconnected, the minimum voltage value is $2.894e-01$. Column 3 contains information on the maximum voltage of phases a, b, and c. Table 2 shows a predetermined number of PMUs with various buses. PMU 1 sets, for example, were installed at buses 2, 6, and 9. PMU 17 refers to the PMUs installed at buses 2, 7, and 9. Bus 30 refers to the PMU installation at buses 2, 6, and 10.

Table 1. The minimum and maximum magnitude of V_{abc} at different buses

PMU placement	Minimum value	Maximum value
Bus 1	1.000e+00	1.191e+05
Bus 2	2.894e-01	1.512e+05
Bus 3	1.000e+00	1.136e+05
Bus 4	1.000e+00	1.144e+05
Bus 5	1.000e+00	1.148e+05
Bus 6	2.894e-01	1.000e+00
Bus 7	1.000e+00	1.193e+05
Bus 8	1.000e+00	1.225e+05
Bus 9	1.000e+00.	1.186e+05
Bus 10	1.000e+00	1.180e+05
Bus 11	1.000e+00	1.189e+05
Bus 12	1.000e+00	1.187e+05
Bus 13	1.000e+00	1.181e+05
Bus 14	1.000e+00	1.162e+05

Table 2. The set of PMU placement

Set of PMU	PMU placement	Set of PMU	PMU placement
1	B2, B6, B9	18	B2, B8, B9
2	B1, B6, B9	19	B2, B10, B9
3	B3, B6, B9	20	B2, B11, B9
4	B4, B6, B9	21	B2, B12, B9
5	B5, B6, B9	22	B2, B13, B9
6	B7, B6, B9	23	B2, B14, B9
7	B8, B6, B9	24	B2, B6, B1
8	B10, B6, B9	25	B2, B6, B3
9	B11, B6, B9	26	B2, B6, B4
10	B12, B6, B9	27	B2, B6, B5
11	B13, B6, B9	28	B2, B6, B7
12	B14, B6, B9	29	B2, B6, B8
13	B2, B1, B9	30	B2, B6, B10
14	B2, B3, B9	31	B2, B6, B11
15	B2, B4, B9	32	B2, B6, B12
16	B2, B5, B9	33	B2, B6, B13
17	B2, B7, B9	34	B2, B6, B14

3.1. Simulation result of LS-SVR

First, the input from table 1 for PMU 1 was entered into the MATLAB software. The random number generator was set to 50. The software yielded hyper-parameters gamma and sigma. The LS-SVR estimate was then obtained using MATLAB software. Figure 7 shows the gamma and sigma values. Estimation of function plotting is based on X and Y values.

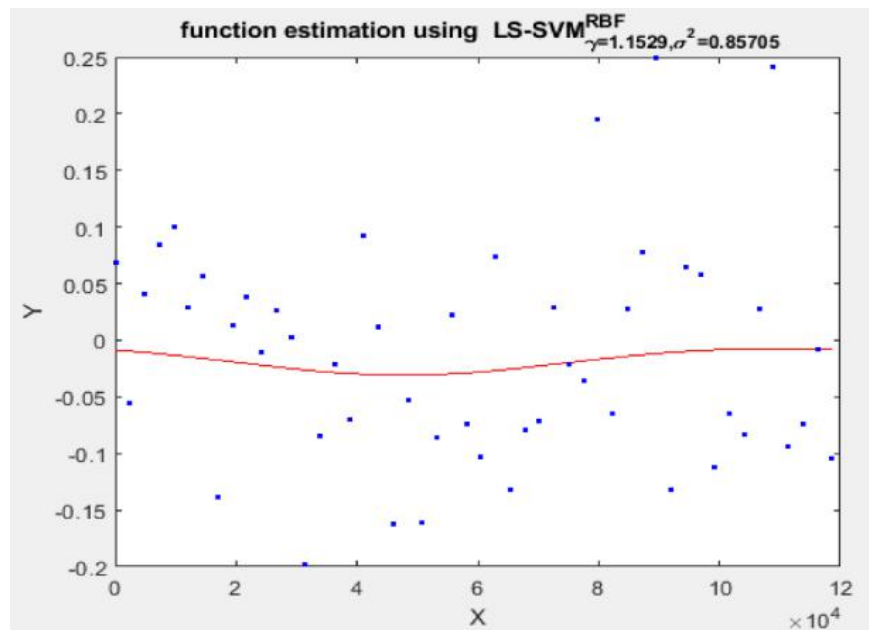


Figure 8. Regression estimation using LSSVR at PMU 1

3.2. MSE

MSE is highlighted as a critical metric that represents the accuracy of PMU placement. Figures 5, 6, and 7 depict the MSE of PMU placement. The MSE is calculated as (11).

$$MSE = \sum \frac{(Y_t - \hat{Y})^2}{Y_t} \quad (11)$$

By considering equation (11), the value of MSE is summarized in Figures 8 to 10.

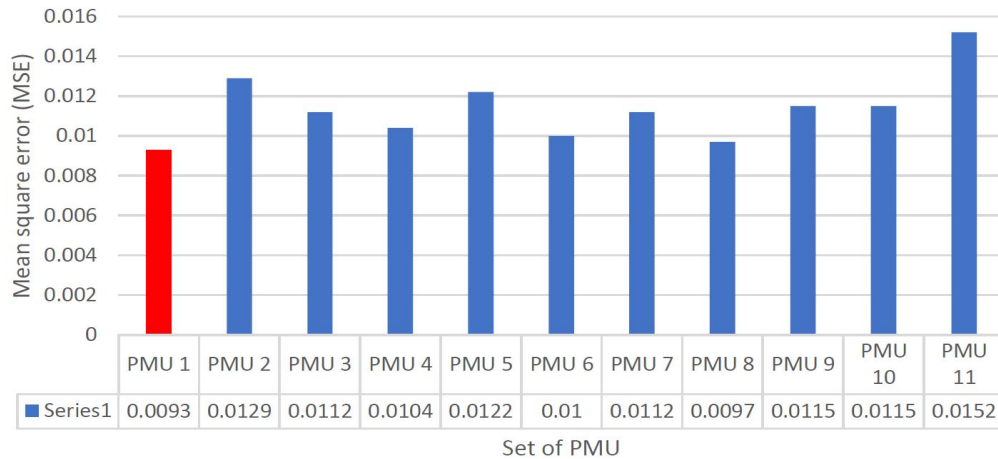


Figure 9. MSE of PMU placement at PMU 1 until PMU 11

The objective of LS-SVR in this study is to determine the accuracy of PMU placement based on MSE. The optimum PMU placement, according to paper [14], is based on the lowest MSE value. The results of this MSE calculation may be summarised using the results of the MSE calculations that have been performed, as shown in Figures 9 to 11. Figure 9 shows how the location of PMUs 1 to 11 resulted in different MSE calculation values, starting with the smallest number, PMU 1 of 0.0093, and progressing to the greatest value, PMU 11 of 0.0152. Figure 10 shows a bar chart displaying the MSE value from PMU 12 to PMU 23. The figure clearly shows that the lowest MSE value was derived from calculations at PMU 23 (0.0095), followed by a larger MSE value, specifically PMU 21 (0.0098), and so on until the MSE value is the greatest at PMU 13 (0.0171).

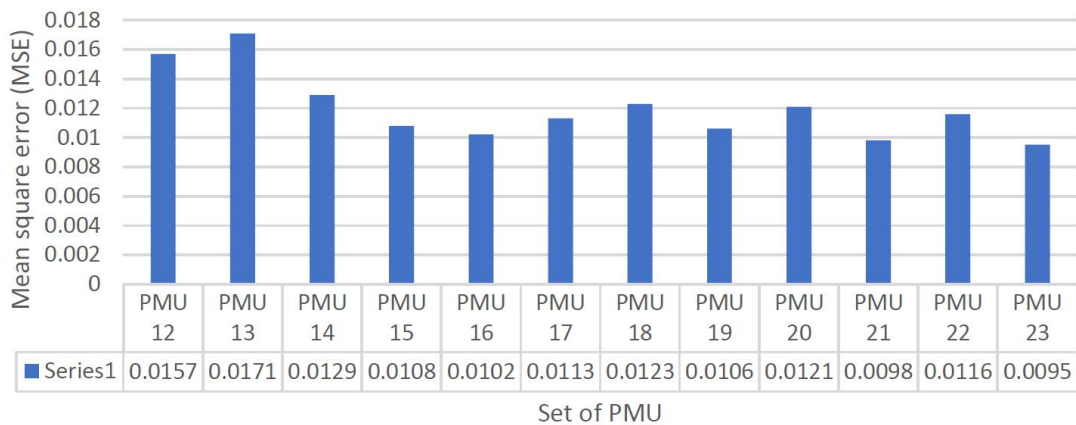


Figure 10. MSE of PMU placement at PMU 12 until PMU 23

Figure 11 depicts the computed MSE values from PMU positions 24 to 34. It can be seen that PMU 30 has the lowest MSE value of 0.0097. The MSE calculation results yielded varied values, as seen in the histogram of Figure 10. Figure 7 depicts the highest MSE value for PMU 29 is 0.0157. In general, the lowest value of each figure may be compared again to make it simpler to draw conclusions in choosing the optimum placement for PMUs. The following equation compares the three lowest values from Figures 5 to 7: PMU 1 (0.0093) < PMU 23 (0.0095) < PMU 30 (0.0097) (12). According to the comparison of the lowest MSE value based on equation 12, the least value of the overall MSE calculation is PMU 1 of 0.0093. As a result, PMU 1 was selected as the optimal location in the IEEE-14 bus system.

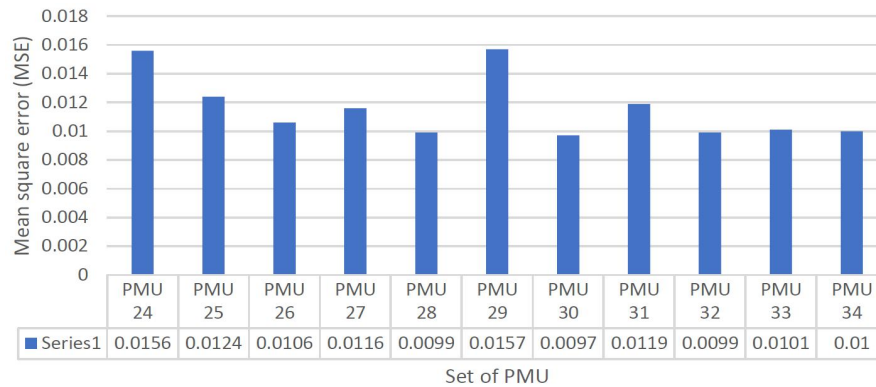


Figure 11. MSE of PMU placement at PMU 24 until PMU 34

4. CONCLUSION

In conclusion, this study proposes control management of a WAMS on the IEEE-14 bus system utilising LS-SVR. PMU 1 recorded the lowest MSE value of 0.0093 when compared to the other set of PMUs. Meanwhile, PMU 13 achieved the highest MSE score of 0.0171. Based on the results obtained, the accuracy of the PMU's placement demonstrated significant improvement when the MSE value was reduced. Based on the lowest value of MSE, it can be concluded that the best placement is at PMU 1.

ACKNOWLEDGEMENTS

The authors thanks to the Airlangga University, Indonesia and SATU Joint Research Scheme (JRS) 2022 no UM22.




REFERENCES

- [1] J. Kim *et al.*, "Study of the effectiveness of a korean smart transmission grid based on synchro-phasor data of K-WAMS," *IEEE Transactions on Smart Grid*, vol. 4, no. 1, pp. 411–418, Mar. 2013, doi: 10.1109/TSG.2013.2240321.
- [2] J. de la Ree, V. Centeno, J. S. Thorp, and A. G. Phadke, "Synchronized phasor measurement applications in power systems," *IEEE Transactions on Smart Grid*, vol. 1, no. 1, pp. 20–27, Jun. 2010, doi: 10.1109/TSG.2010.2044815.
- [3] A. Ghasemkhani, H. Monsef, A. R. Kian, and A. A. Moghaddam, "Optimal design of a wide area measurement system for improvement of power network monitoring using a dynamic multiobjective shortest path algorithm," *IEEE Systems Journal*, vol. 11, no. 4, pp. 2303–2314, Dec. 2017, doi: 10.1109/JSYST.2015.2469742.
- [4] R. Gore and M. Kande, "Analysis of wide area monitoring system architectures," in *2015 IEEE International Conference on Industrial Technology (ICIT)*, 2015, vol. 2015-June, no. June, pp. 1269–1274, doi: 10.1109/ICIT.2015.7125272.
- [5] J. Cepeda, D. Echeverria, and G. Arguello, "Cenace's experiences on implementing a wide area monitoring system (WAMS) in the Ecuadorian power system," in *2014 IEEE Central America and Panama Convention (CONCAPAN XXXIV)*, 2014, pp. 1–7, doi: 10.1109/CONCAPAN.2014.7000455.
- [6] M. M. Eissa, M. M. Elmesalawy, and M. M. A. Hadhoud, "Wide area monitoring system based on the third generation universal mobile telecommunication system (UMTS) for event identification," *International Journal of Electrical Power & Energy Systems*, vol. 69, pp. 34–47, Jul. 2015, doi: 10.1016/j.ijepes.2014.12.077.
- [7] A. B. Leirbukt, J. O. Gjerde, P. Korba, K. Uhlen, L. K. Vormedal, and L. Warland, "Wide area monitoring experiences in Norway," in *2006 IEEE PES Power Systems Conference and Exposition*, 2006, pp. 353–360, doi: 10.1109/PSC.2006.296331.
- [8] W. Liu, Z. Lin, F. Wen, and G. Ledwich, "A wide area monitoring system based load restoration method," *IEEE Transactions on Power Systems*, vol. 28, no. 2, pp. 2025–2034, May 2013, doi: 10.1109/TPWRS.2013.2249595.
- [9] M. Qiu, W. Gao, M. Chen, J.-W. Niu, and L. Zhang, "Energy efficient security algorithm for power grid wide area monitoring system," *IEEE Transactions on Smart Grid*, vol. 2, no. 4, pp. 715–723, Dec. 2011, doi: 10.1109/TSG.2011.2160298.
- [10] L. J. Awalín, H. Mokhlis, M. K. Rahmat, S. Shilpa, F. Albatsh, and B. Ismail, "Fault distance identification using impedance and matching approaches on distribution network," *Indonesian Journal of Electrical Engineering and Computer Science*, vol. 8, no. 3, p. 770, Dec. 2017, doi: 10.11591/ijeecs.v8.i3.pp770-778.
- [11] L. J. Awalín, T. Tien, T. Lea, and H. Suyono, "Comparison study of fault location on distribution network using PSCAD and DIGSILENT power factory by using matching approaches," *Indonesian Journal of Electrical Engineering and Computer Science*, vol. 17, no. 1, pp. 78–85, 2020, doi: 10.11591/ijeecs.v17.i1.pp78-85.
- [12] M. H. Idris, M. R. Adzman, H. Mokhlis, M. F. Naim Tajuddin, H. Hamid, and M. Amiruddin, "Two-terminal fault detection and location for hybrid transmission circuit," *Indonesian Journal of Electrical Engineering and Computer Science*, vol. 23, no. 2, p. 639, Aug. 2021, doi: 10.11591/ijeecs.v23.i2.pp639-649.
- [13] L. J. Awalín, F. Fatini, M. N. Abdullah, L. T. Tay, M. F. A. Hamid, and B. Ismail, "Voltage & Current magnitude pattern recognition by using fuzzy logic toolbox for fault types classification," *Indonesian Journal of Electrical Engineering and Computer Science*, vol. 12, no. 1, p. 326, Oct. 2018, doi: 10.11591/ijeecs.v12.i1.pp326-332.
- [14] Y. Wang, W. Li, J. Lu, and H. Liu, "Evaluating multiple reliability indices of regional networks in wide area measurement system," *Electric Power Systems Research*, vol. 79, no. 10, pp. 1353–1359, Oct. 2009, doi: 10.1016/j.epsr.2009.04.005.





- [15] F. H. Fesharaki, R.-A. Hooshmand, and A. Khodabakhshian, "Simultaneous optimal design of measurement and communication infrastructures in hierarchical structured WAMS," *IEEE Transactions on Smart Grid*, vol. 5, no. 1, pp. 312–319, Jan. 2014, doi: 10.1109/TSG.2013.2260185.
- [16] T. Qian, H. Xu, J. Zhang, A. Chakraborty, F. Mueller, and Y. Xin, "A resilient software infrastructure for wide-area measurement systems," in *2016 IEEE Power and Energy Society General Meeting (PESGM)*, 2016, vol. 2016-Novem, pp. 1–5, doi: 10.1109/PESGM.2016.7741949.
- [17] C. Cyr, I. Kamwa, R. O'Reilly, and S. Rolle, "Development and Testing of Phasor Data Concentrators for a Wide-Area Control System," in *In Proc. 37th Annu. Western Protect. Relay Conf. (WPRC)*, 2010, pp. 1–13.
- [18] S.-E. Razavi, H. Falaghi, and M. Ramezani, "A new integer linear programming approach for multi-stage PMU placement," in *2013 Smart Grid Conference (SGC)*, 2013, pp. 119–124, doi: 10.1109/SGC.2013.6733822.
- [19] B. Gou, "Optimal placement of PMUs by integer linear programming," *IEEE Transactions on Power Systems*, vol. 23, no. 3, pp. 1525–1526, Aug. 2008, doi: 10.1109/TPWRS.2008.926723.
- [20] K. S. K. Reddy, D. A. K. Rao, A. Kumarraja, and B. R. K. Varma, "Implementation of Integer Linear Programming and Exhaustive Search algorithms for optimal PMU placement under various conditions," in *2015 IEEE Power, Communication and Information Technology Conference (PCITC)*, 2015, pp. 850–855, doi: 10.1109/PCITC.2015.7438114.
- [21] A. Almunif and L. Fan, "Mixed integer linear programming and nonlinear programming for optimal PMU placement," in *2017 North American Power Symposium (NAPS)*, 2017, pp. 1–6, doi: 10.1109/NAPS.2017.8107398.
- [22] M. B. Mohammadi, R.-A. Hooshmand, and F. H. Fesharaki, "A new approach for optimal placement of PMUs and their required communication infrastructure in order to minimize the cost of the WAMS," *IEEE Transactions on Smart Grid*, vol. 7, no. 1, pp. 84–93, Jan. 2016, doi: 10.1109/TSG.2015.2404855.
- [23] A. Kumar and S. Bhongade, "A novel approach for placement of Phasor Measurement Unit & counting their optimal number," *Electrical and Electronics Engineering: An International Journal*, vol. 5, no. 1, pp. 73–80, Feb. 2016, doi: 10.14810/eel.2016.5106.
- [24] R. F. Nuqui and A. G. Phadke, "Phasor measurement unit placement techniques for complete and incomplete observability," *IEEE Transactions on Power Delivery*, vol. 20, no. 4, pp. 2381–2388, Oct. 2005, doi: 10.1109/TPWRD.2005.855457.
- [25] J. Pahasa and I. Ngamroo, "Least squares support vector machine for power system stabilizer design using wide area phasor measurements," *International Journal of Innovative Computing, Information and Control*, vol. 7, no. 7 B, pp. 4487–4501, 2011.
- [26] A. G. Phadke and J. S. Thorp, "Control with Phasor Feedback," in *Synchronized Phasor Measurements and Their Applications*, New York: Springer, 2017, pp. 185–209.
- [27] Y. Zhang *et al.*, "Wide-area frequency monitoring network (FNET) architecture and applications," *IEEE Transactions on Smart Grid*, vol. 1, no. 2, pp. 159–167, Sep. 2010, doi: 10.1109/TSG.2010.2050345.
- [28] J. A. K. Suykens, B. Baesens, S. Viaene, J. Vanthienen, G. Dedene, and J. Vande, "Benchmarking least squares support vector machine classifiers," *Machine Learning*, vol. 54, no. 1, pp. 5–32, 2004.
- [29] J. A. K. Suykens, T. van Gestel, J. de Brabanter, B. de Moor, and J. Vandewalle, *Least Squares Support Vector Machines*. K U Leuven: Wolrd Scientific, 2002.
- [30] J. A. K. Suykens and J. Vandewalle, "Least squares support vector machine classifiers," *Neural Processing Letters*, vol. 9, no. 3, pp. 293–300, 1999, doi: 10.1023/A:1018628609742.
- [31] G. Gangil and R. Narvey, "Advanced security algorithm for power grid," in *2013 International Conference on Communication Systems and Network Technologies*, 2013, pp. 409–417, doi: 10.1109/CSNT.2013.92.
- [32] F. Cao and Y. Yuan, "Learning errors of linear programming support vector regression," *Applied Mathematical Modelling*, vol. 35, no. 4, pp. 1820–1828, Apr. 2011, doi: 10.1016/j.apm.2010.10.012.
- [33] V. N. Vapnik, *The nature of statistical learning theory*. New York, NY: Springer New York, 2000.
- [34] K. de Brabanter, J. de Brabanter, J. A. K. Suykens, and B. de Moor, "Approximate confidence and prediction intervals for least squares support vector regression," *IEEE transactions on neural networks*, vol. 22, no. 1, pp. 110–20, Jan. 2011, doi: 10.1109/TNN.2010.2087769.
- [35] R. M. Adnan *et al.*, "Air temperature prediction using different machine learning models," *Indonesian Journal of Electrical Engineering and Computer Science*, vol. 22, no. 1, p. 534, Apr. 2021, doi: 10.11591/ijeecs.v22.i1.pp534-541.
- [36] G. Gordon and R. J. Tibshirani, "Karush–kuhn–tucker conditions," *Optimization*, p. 26, 2012.
- [37] K.-M. Jung, "Support vector regression with the weighted absolute deviation error loss function," *Journal of the Korean Data And Information Science Society*, vol. 29, no. 6, pp. 1707–1719, Nov. 2018, doi: 10.7465/jkdi.2018.29.6.1707.
- [38] W. Wen, Z. Hao, and X. Yang, "Robust least squares support vector machine based on recursive outlier elimination," *Soft Computing*, vol. 14, no. 11, pp. 1241–1251, Sep. 2010, doi: 10.1007/s00500-009-0535-9.
- [39] L. A. Kumar and S. Karthikeyan, "Modeling of phasor measurement unit for wide area monitoring and control of smart grids with distributed energy resources," in *2016 IEEE Conference on Technologies for Sustainability (SusTech)*, 2016, pp. 188–194, doi: 10.1109/SusTech.2016.7897165.
- [40] V. Centeno, J. de la Ree, A. G. Phadke, G. Michel, R. J. Murphy, and R. O. Burnett, "Adaptive out-of-step relaying using phasor measurement techniques," *IEEE Computer Applications in Power*, vol. 6, no. 4, pp. 12–17, Oct. 1993, doi: 10.1109/67.238199.

BIOGRAPHIES OF AUTHORS







Lilik Jamilatul Awal    was born in East Java, Indonesia, in 1977. She received the B. Eng. degree in electrical engineering in 1999 from the University of Widya Gama, M.Eng. degree in 2004 from the Institut Teknologi Sepuluh Nopember, Indonesia and Ph.D. degree in 2014 from University of Malaya. She was a Senior Lecturer in 2015–2020 in University Kuala Lumpur, Electrical Engineering Section, British Malaysia Institute, Batu 8, Jalan Sg. Pusu, 53100, Gombak Selangor, Malaysia. Currently, she is a senior lecturer in Airlangga University, Indonesia. Her research interest includes fault location, protection system, distribution and transmission system, smart grid. She can be contacted at email: lilik.j.a@ftmm.unair.ac.id.







Syahirah Abd Halim     received the bachelor's degree in Electrical & Electronics Engineering from Universiti Teknologi Petronas, Perak in 2009. She received the master's degree and the Ph.D. degree in Electrical Engineering from the University of Malaya, Kuala Lumpur, in 2012 and 2016 respectively. She joined UM Power Energy Dedicated Advanced Centre as a Postdoctoral Research Fellow in January 2017. Since August 2017, she has been a Senior Lecturer with the Department of Electrical, Electronic and Systems Engineering, Universiti Kebangsaan Malaysia. Her research interests include transmission line modelling, transient analysis and optimization techniques. She can be contacted at email: syahirah_h@ukm.edu.my.







Nor Azuana Ramli     is senior lecturer at Centre of Mathematical Sciences, Universiti Malaysia Pahang. Received Ph.D. from Universiti Sains Malaysia, Master in Innovation & Engineering Design from Universiti Putra Malaysia and BSc degree in Mathematical Industry from Universiti Teknologi Malaysia. Research involving data analysis, machine learning, applied statistics and data mining. She can be contacted at email: azuana@ump.edu.my.



Jafferi Bin Jamaludin     received the B.Eng. degree from Universiti Tenaga Nasional, Putrajaya, Malaysia and M.Eng.Sc. and Ph.D. degrees from University of Malaya, Kuala Lumpur, Malaysia. He is currently a Senior Lecturer at the University of Malaya Power Energy Dedicated Advanced Centre (UMPEDAC). In 2018, he received a scholarship from the Hitachi Global Foundation to carry out postdoctoral research at Keio University, Japan for 12 months. In 2017, he participated in an energy manager training program endorsed by the Energy Commission Malaysia. Since 2018, Dr. Jafferi has been recognized as a Professional Technologist registered with Malaysia Board of Technologists (MBOT) in the field of electrical and electronics technology. He is a member of the Institute of Electrical and Electronics Engineers, USA. He can be contacted at email: jafferi@um.edu.my.



Mohd Syukri Ali     received his bachelor's degree in Telecommunication Engineering from Universiti Malaya, Kuala Lumpur in 2009. He further his master's degree and Ph.D. degree in Power System from the Universiti Malaya, Kuala Lumpur, in 2013 and 2018 respectively. He joined UM Power Energy Dedicated Advanced Centre as a Postdoctoral Research Fellow in November 2018 and later become a Research Officer in November 2019. His research interests include power system analysis, digital signal processing, artificial intelligent and optimization techniques. He can be contacted at email: syukriali@um.edu.my.